

## **Influence of Steel Fiber Size and Shape on Quasi-Static Mechanical Properties and Dynamic Impact Properties of Ultra-High Performance Concrete**

Dylan A. Scott<sup>1</sup>, Wendy R. Long, Robert D. Moser, Brian H. Green, James L. O’Daniel, and Brett A. Williams

<sup>1</sup> Geotechnical and Structures Laboratory; Army Engineer Research and Development Center; 3909 Halls Ferry Road; Vicksburg, MS 39180-6199

### **Abstract**

This investigation focused on identifying the impact of various steel fiber types on the mechanical response of an ultra-high performance concrete (UHPC) known as Cor-Tuf (CT). CT specimens were fabricated with four steel fiber types: hooked-end 3D 55/30 BG fibers, undulated NYCON type V fibers, straight brass coated OL 10mm fibers, and straight brass coated OL 6mm fibers. Fiber shape and size had a limited impact on quasi-static properties in compression but had a significant impact on quasi-static tensile properties and dynamic penetration resistance. The use of smaller fibers resulted in up to a 100 percent increase in component/test article tensile strength compared with their larger fiber size counterparts. However, the benefits offered by the smaller fibers primarily occurred prior to reaching the ultimate load carrying capacity. Once the ultimate strength was reached, larger fibers were more effective at bridging larger cracks. Smaller fibers provided improved penetration resistance, with reduced residual projectile velocities and loss of material from cratering and/or spallation. The overall goal of the study was to identify the relationships between fiber characteristics and the multi-strain rate response of UHPCs in order to better optimize fiber reinforcement for various loading conditions.

Keywords: Ultra-High Performance Concrete, steel fiber reinforcement, Impact behavior,

Mechanical testing

## 1 Introduction

Ultra-high performance concrete (UHPC) is a family of materials that typically exhibit compressive strengths in excess of 150 MPa (21,000 psi) and high durability due to negligible interconnected porosity. High toughness is achieved with the addition of fiber reinforcement (Burroughs, J. et al 2013). UHPC formulations generally consist of a high cementitious content incorporating oil-well or low-heat portland cement (i.e., with large mean particle size, high C2S content, and low C3A content), siliceous or aluminous fine aggregates, crushed quartz or some other micrometer-sized powder, silica fume, water, high-range water-reducing admixtures to control rheology, and other components that vary by manufacturer (Burroughs, J. et al 2013). With the high compressive strengths of UHPC comes brittle behavior similar to that of a ceramic material. To overcome this brittle behavior, steel fiber reinforcement is commonly used (Williams, B.A. 2015). The addition of steel fiber reinforcement aids in delocalizing micro- and macro-scale cracking and leads to improvements in tensile properties (e.g., tensile strength and flexural response) and minimized spallation during failure (Green, B. et al. 2014).

Various UHPC formulations exist, with the majority being developed by manufacturers. The matrices (i.e., the portions of the UHPC excluding the fiber reinforcement) are generally similar in composition and basic mechanical properties. The variations observed in UHPC failure morphology when subjected to extreme loading events are hypothesized to largely be related to the steel fiber reinforcement—including its strength, length and diameter as well as and any deformations present that provide mechanical interlock with the matrix.

### 1.1 Cor-Tuf

As previously described, many UHPC formulations exist, including those available from commercial vendors and those developed in-house. Cor-Tuf (CT) is one formulation of UHPC developed by engineers at the U.S. Army Engineer and Research Development Center (ERDC) under the name Cor-Tuf. This family of UHPCs is a result of more than three decades of work and investigation into the use of UHPCs and the creation of subsequent adaptations to better suit the material for a variety of applications for both military and civil infrastructures (Green, B. et al. 2014).

Green et al. (2014) detailed CT as being “developed to serve as, and is currently considered by ERDC to be, a ‘laboratory standard’ UHPC mixture, that can be reproduced for various projects and exhibit the same physical properties with minimal batch-to-batch variability” (O’Neil 2008). CT’s constituent materials (excluding fibers) include a Class H oil well cement, silica fume, silica sand, crushed silica sand (also known as silica flour), and a polycarboxylate type high-range water-reducing admixture (HRWRA) (Williams, E. et al. 2009). These are brand specified materials at specified proportions that allow for a highly reproducible mixture with little variability between mixtures. Table 1 shows the mixture proportions for CT.

**Table 1. CT mixture proportion.**

Material	Proportion by Weight
Cement	1.00
Silica Fume	0.389
Silica Flour	0.277
Silica Sand	0.967
HRWRA	0.0171
Water	0.208
Steel Fibers	0.310

CT typically has an unconfined compressive strength (UCS) between 193 to 220 MPa (28 to 32ksi) and a density of approximately 2563 kg/m<sup>3</sup> (160 lb/ft<sup>3</sup>). With this high strength, CT (as

well as most other UHPCs) has a high brittleness that can be counteracted by the inclusion of randomly distributed steel fibers.

Up to this point, the only steel fiber included in CT was the ZP 305 fiber produced by the Bekaert Corporation. This fiber has recently been renamed as 3D 55/30 BG fiber in order to coincide with the Bekaert Corporation's recently released brands of fibers. The fiber itself is 0.55 mm (0.022 in.) in diameter and 30 mm (1.18 in.) in length with hooked ends and is included into CT mainly because of its relatively low cost and easy attainability. Mechanical testing performed by Roth et al. (2010) compared the compressive, flexural, and splitting tensile properties of CT with and without the inclusion of the 3D 55/30 BG fibers. The results of this testing showed that when steel fibers were included in the Cor-Tuf matrix, a slight increase occurred in compressive strength, a 162 percent increase occurred in flexural strength, and a 240 percent increase occurred in splitting tensile strength. An improvement in the mode of failure was also observed. CT without fibers resulted in a catastrophic and brittle failure as opposed to the CT with fiber matrix that held together after fracture and absorbed more energy.

These results proved that a randomly distributed steel fiber-reinforced UHPC matrix is far superior to a UHPC matrix without fibers. However, little to no work has been done to provide insight into how the size and shape of steel fiber reinforcement could change the mechanical behavior of a UHPC matrix as a whole.

## 2 Experimental Program

All tested specimens utilized a consistent UHPC matrix of the CT formulation shown in Table 1. Keeping the UHPC matrix constant ensured that a direct comparison could be made between fiber types. Part of this procedure included a consistent curing regime and testing age of each of the four test matrices. The curing regime consisted of seven days of 22°C curing inside a fog room with 100 percent humidity followed by seven days of steam curing at a temperature of 90°C (190°F). The testing age of each CT matrix was between 26 and 29 days. The slight variance in age was due to the large amount of testing that was conducted and the limited amount of testing equipment. This age variance should have little effect on test results.

Testing of specimens was performed at quasi-static and dynamic strain rates using the methods described in the following sections. The overall scope of the experimental program is shown in Table 2.

**Table 2. Overview of experimental program.**

Test Method	Notes
Compressive Strength	Unconfined compressive strength of 10.16- by 20.32-cm cylinders (4-by-8-in.)
Flexural Response	Flexural testing of 15.24- by 15.24- by 53.34-cm. beams (6-by-6-by-21-in.)
Direct Tensile Testing	Direct tensile testing of water-jet cut-out and cast dog bone samples
FSP / Penetration	FSP testing of 5.08-cm., 6.35-cm., and 7.62-cm.-thick panels (2-in., 2.5-in., and 3-in.)

### 2.1 Steel fiber types

This section will discuss all of the fiber types, the intent of their design, and their possible effects on the CT matrix. The fibers included in this report are the 3D 55/30 BG (Bekaert Co.), the Nycon Type V (Nycon Co.), the OL 0.2/10 mm, and the OL 0.16/6 mm (Bekaert Co.).

The 3D 55/30 BG fiber previously discussed is currently the standard fiber used in the CT matrix. This fiber is 30 mm long and 0.5 mm in diameter. The hooked ends of these fibers are designed to “anchor” into the concrete specimen; and, as the specimen fractures, these

hooks/anchors cause the fiber to stretch and eventually fail under tension in the midsection of the fiber.

The length and size of the 3D 55/30 BG fibers lead to a low volume density of fibers, which increases the nearest neighbor space to the next fiber. This could allow cracking to propagate uninhibited across a greater length when compared to a smaller fiber with a higher volume density, which may result in lower tensile strengths. However, the larger size and shape should also make it more likely that a UHPC containing these fibers will be able to maintain its integrity post failure.

The Nycon Type V is an undulated (wavy) low-carbon steel fiber, which is 38 mm (1.5in) long and has a 1.18-mm (0.046-in.) filament. Instead of using the hooked ends to anchor the fiber, the waves are designed to straighten as the matrix begins to fail and the fiber begins to pull out. These waves result in higher fiber pullout strengths that allow for more slippage, thus making the entire material more ductile.

The next two fiber types are small, straight, brass-coated steel fibers. The Bekaert OL .2/10mm fiber is 0.2 mm (0.008 in.) in diameter and is 10 mm (0.39in.) in length. The Bekaert OL .16/6mm fiber was 0.16 mm (0.0063 in.) in diameter and 6 mm (0.24 in.) in length. The possible advantages of these fibers are their high surface area and small volume. Since fiber dosages are made on a standard percent by weight basis, replacement of larger fibers such as 3D 55/30 BGs with smaller OL fibers results in a greater density of fibers dispersed in the UHPC matrix. The high-surface areas make it more likely that, upon failure, the crack propagation will encounter several fibers and possibly stop the fracture. The disadvantage of these fibers is their short length. The shorter lengths make the fiber unable to “bridge” a large crack upon significant damage. These shorter OL fibers could be beneficial in the micro-cracking regime, but their inability to bridge a macro-crack likely limits their effectiveness.

Fiber costs are important to consider. The Nycon fibers are the least expensive, while the OL fibers are the most expensive at about 3 dollars per kilogram (one dollar per pound) more than the 3D 55/30 BG fibers. Therefore, it will be hard to fiscally justify use of the OL fibers. However, single companies provided these costs, and it is likely possible to find different sources with lower costs.

## **2.2 *Experimental methods***

### **2.2.1 Compression: Strength**

The UCS and elastic modulus testing was performed to ensure that each CT matrix met the first condition of the testing procedure. These test methods and all subsequent test methods were followed strictly and consistently to ensure that the second testing condition was met. The UCS was conducted according to ASTM C873 (ASTM International 2010a).

### **2.2.2 Flexural response**

Flexural response testing was performed according to ASTM C1609 (ASTM International 2012). This test used a beam with four-point loading. The cast beams were 150 by 150 by 500 mm (6 by 6 by 21 in.) and were cast according to ASTM C192 (ASTM International 2013). They were tested on a 450-mm (18-in.) support span in 4-point bending with loading points positioned at 1/3<sup>rd</sup> positions along the supported span. Linear variable differential transformers (LVDTs) were used to measure center-line displacement that was in turn paired with the corresponding load data to provide a plot of load versus displacement.

### **2.2.3 Direct tensile testing**

The direct tensile testing (DTT) is an ERDC-specific test that was adapted from a 2008 Japanese Society of Civil Engineers, Concrete Engineering Series 82 (JSCE 2008). This testing procedure

consists of taking a dog-bone-shaped specimen with cross-sectional dimensions of 1.18 by 1.18 in. (30 by 30 mm) in the gage length and applying a constant specimen deformation rate of approximately 0.02 in. (0.5 mm)/min with two LVDTs on diagonally opposite corners of the gage length in order to capture the complete displacement in all directions. Each specimen was tested with a gage length of 4 in. (101.6 mm).

Nine dog-bone specimens were made in two different methods. First, four specimens were cast in molds with the specified dog-bone shape. This method proved easy and effective during placement; however, fiber-alignment became a real concern particularly for fibers with lengths in excess of 25mm (1 in.). The molds caused the fibers to align along the axis that the tensile stress would be applied during testing. This could result in a tendency for higher DTT strengths. The second method consisted of casting large flexural beams, cutting slabs from these beams to the specified thickness, and using a water jet to cut out the dog-bone shape from the slabs. Five samples for each fiber type were made using this method.

Figure 3 shows the actual direct tensile testing configuration pretest and posttest, respectively. This configuration utilized a chucking mechanism suited to the shape of each specimen and was designed to allow tensile loading along the specimen's central axis. The top chuck utilized one rotational degree of freedom to allow better vertical alignment, while the bottom chuck utilized a torsional degree of freedom to prevent torsional stresses caused by possible grip misalignment.

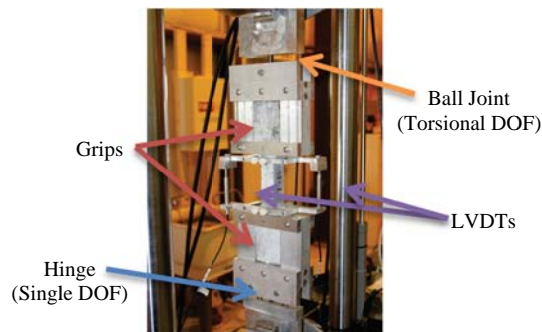


**Figure 3. DTT testing configuration (adapted from JSCE 2008).**

#### 2.2.4 Dynamic penetration using fragment simulating projectiles

Direct fire experiments were conducted using a 0.50-caliber fragment simulating projectile (FSP) to examine the resistance of the UHPC panels to small projectile penetration. A single projectile was fired at each panel with approximately the same impact velocity in each test. Each direct fire experiment measured impact velocity, the residual velocity of the projectile in the event of perforation, and the final damage state of the target. Samples of the UHPC panels were cast to a uniform 30.5 mm by 30.5 mm (12-in. by 12-in) size with thicknesses of 2.54-cm, 5.08-cm., 6.35-cm., and 7.62-cm. (1.0, 2.0, 2.5, and 3.0 in). A set of three panels was generated for each thickness. The desired impact velocity was approximately 1067m/sec (3,500 ft/sec). This combination of panel thicknesses and impact velocity was chosen because it had previously generated damage states and responses that varied from complete perforation of the panel to only cratering of the impact side of the panel (Reinhart and Thornhill 2010). All direct fire experiments were conducted in ERDC's small-arms ballistic testing facility. The range from muzzle to target in this experimental program was approximately 4.57 m (15 ft).

Projectile velocity measurements were made using a set of Oehler Research, Inc. Model 35P proof chronographs, each connected to two Oehler Model 55 light screens. The light screens attached to each chrono- graph were positioned 0.91 (3 ft) apart to capture projectile velocities. Four chronograph screens were positioned between the gun and the target to estimate the impact

velocity. The velocity was measured between pairs of the screens, and an estimated impact velocity was generated for each test based on these measurements. A single pair of screens was positioned approximately 1.22m (4 ft) behind the test specimens to measure exit (residual) velocities for each experiment. All experiments were conducted with 0-deg obliquity.

### 3 Quasi-Static Test Results and Discussion

#### 3.1 Compressive strength

As discussed in the testing procedures section, the UCS results were used to verify that each CT matrix was consistent so that a direct comparison could be made between steel fiber types. Table 4 shows the results of the ASTM C873 (ASTM International 2010a) testing. It can be seen that all of the compressive strengths are similar.

**Table 4. ASTM C873 UCS testing results.**

Fiber Type	Unconfined Compressive Strength (MPa)			
	ZP305	NYCON	OL 6 mm	OL 10 mm
3 Sample Avg.	202.5	178.4	209.0	215.9

UHPC specimens containing the Nycon fibers resulted in slightly lower strengths of about 26 ksi (179 MPa). There are several potential reasons for this occurrence: possible batching errors, possible cylinder casting errors, or the size of the fiber itself. It is not believed that the lower strength is as a result of the fiber.

#### 3.2 Flexural response

The ultimate flexural strengths for each fiber type were compared to that matrix's corresponding UCS and were expressed as a percentage of UCS. Each fiber type's ultimate flexural strength ranged between 10 and 11 percent. Figure 7 shows these results as plots of applied load versus center-line displacement.

The difference between these fiber types can be clearly seen in Figure 7. Toughness is the ability of a material to absorb energy and is defined by ASTM C1609 (ASTM International 2012) as being the area under the flexural strength curve up to  $L/150$ , where  $L$  is the support span length. The OL 6mm fibers mixture failed in a brittle manner. The sharp drop upon failure means this material has a low toughness, and it is likely failing this way because the short length of the fiber is unable to "bridge" the larger cracks and hold the matrix together. In the case of the OL 10mm fibers with similar shape and aspect ratio but larger overall size, the flexural response exhibited higher nonlinearity near the maximum strength. Results from the 3D 55/30 BG and Nycon fibers suggest that, as fiber sizes become longer, post yield load carrying capacity and toughness actually increase.

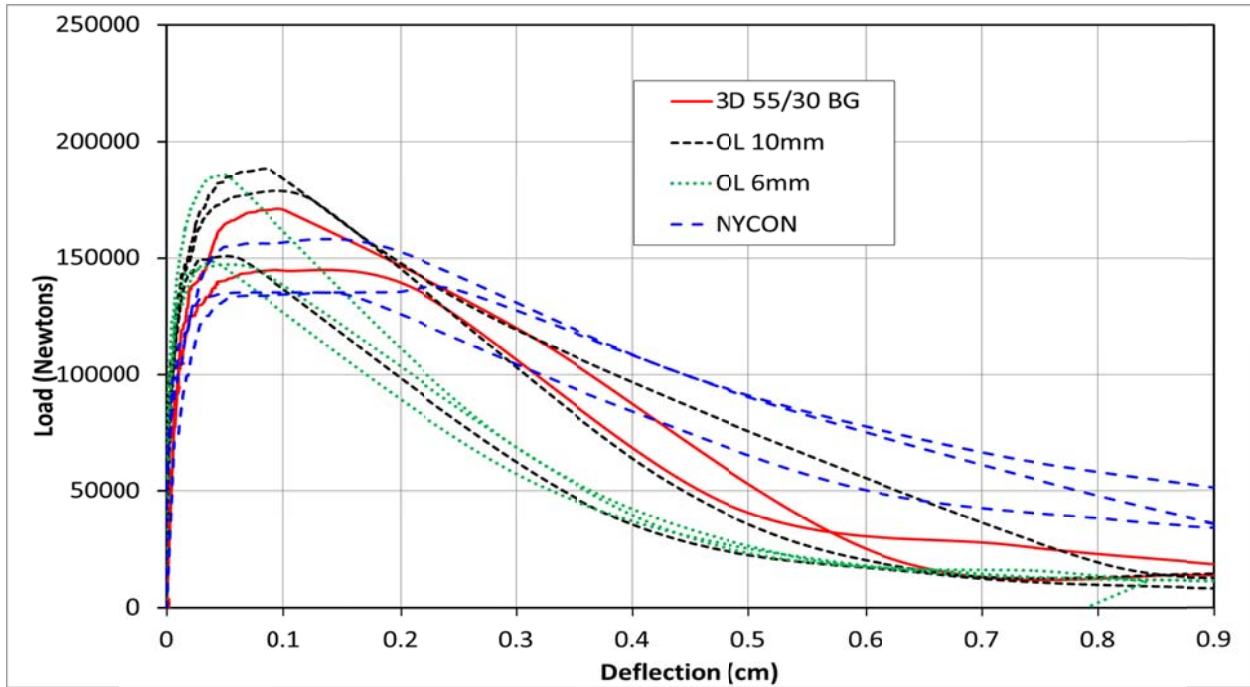


Figure 7. Flexural response Load in newtons vs. Deflection in centimeters as measured on the tensile face with LVDTs.

### 3.3 Direct tensile testing

Figure 8 shows the stress-strain responses observed in DTTs for samples that were cast into dog-bone shaped molds. The stress-strain responses for the samples cut using a waterjet were very similar, but with lower peak stresses. Summaries of the results are provided in Tables 7 and 8. Multiple exclusions were made in each Table to address sample defects such as: uneven distribution of fiber in the vicinity of failure, for no fiber bridging the crack, minimal fibers bridging the crack, and large air voids near the edge of the gage length. Figure 10 provides a comparison of all the data.

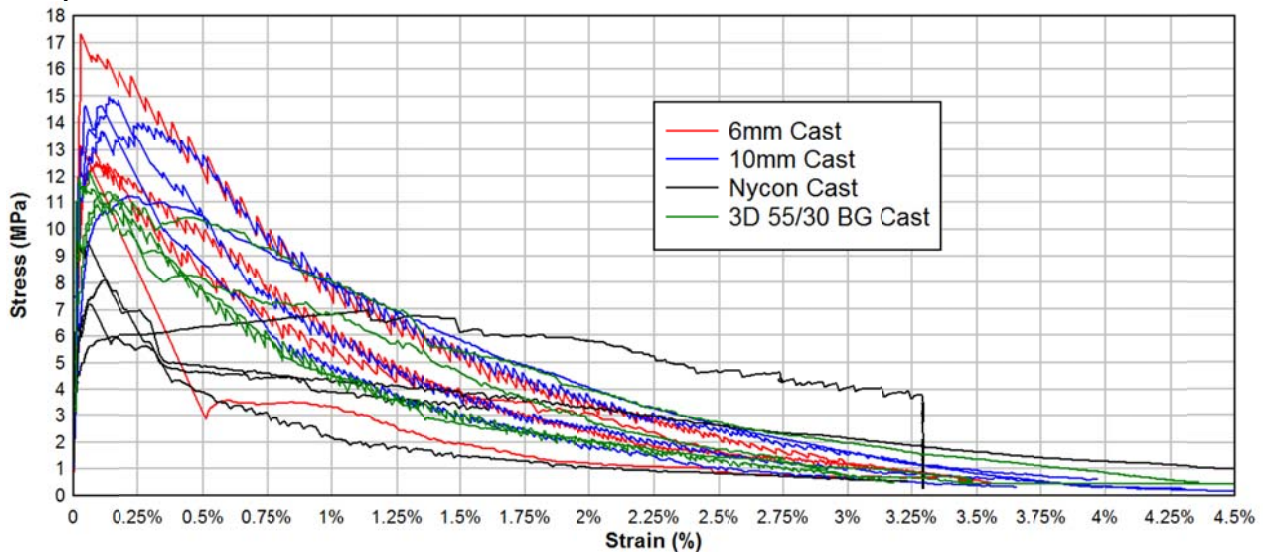


Figure 8. Stress vs. strain DTT results for mold-cast specimens that exhibited longitudinal fiber orientation.

**Table 7. DTT peak results from specimens cast in molds.**

Specimen	Tensile Strength (kN)			
	6 mm	10 mm	Nycon	ZP 305
Average of 4 dog-bones	12.61	12.20	7.16	10.47
Average excluding Imperfections	12.61	12.89	7.16	10.47

**Table 8. DTT peak results from specimens cut using a waterjet from larger flexural beams.**

Specimen	Tensile Strength (kN)			
	6 mm	10 mm	Nycon	ZP 305
Average of 5 dog-bones	12.82	9.16	3.83	5.74
Average excluding Imperfections	12.82	9.83	4.62	8.12

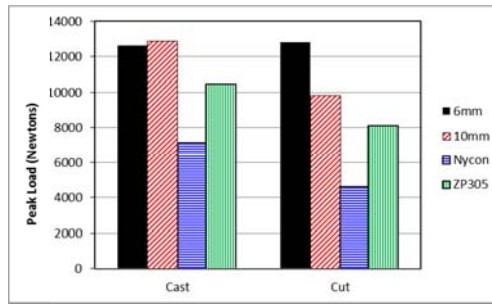


**Figure 10. Summary of DTT results with comparison between specimens that were cast vs. those that were cut from larger flexural beams.**

In both the cast and the cut specimens, there was a clear trend in the relationship between fiber size and tensile behavior. The smaller OL 6mm fibers exhibited the highest strength and stress vs. strain linearity. As fiber size increased, tensile strength, as well as toughness, reduced significantly. The two largest fibers, Nycon Type V and 3D 55/30 BG, exhibited the lowest strengths and extremely low toughness with rapid reductions in load carrying capacity following the ultimate stress peak.

Issues associated with fiber alignment are also easily seen in these results, which provide a direct comparison between the two methods of preparation. Higher tensile strengths occurred from the cast specimens versus the water-jetted samples in all fibers except for the Bekaert 6 mm. The strengths for the Bekaert 6 mm cast and cut specimens were similar and were the least affected by the small specimen size.

In addition, the effect of fiber loading by weight or volume percentage vs. by number of fibers is also clearly a factor, as many of the defects observed during testing were attributed to a lack of fibers crossing the plane of failure. For example, when examined following testing, many of the Nycon Type V and 3D 55/30 BG specimens had no fibers bridging the fracture plane. The smaller OL fibers, since they are far greater in number, more easily bridged the fracture plane.

While the results do generally suggest that smaller fibers help to improve tensile strengths in UHPC, the issues associated with fiber size vs. sample size are significant. For instance, larger fibers could exhibit a higher toughness if sample sizes were increased, and fiber alignment issues would dissipate. Tests on much larger specimens are necessary to better predict tensile properties and minimize the effects of preferential fiber orientation during sample fabrication.

#### 4 Dynamic Testing Results and Discussion

Each panel was impacted with an FSP and resulted in damage. In each case, fibers were exposed with some only on the impact side of the panel and others on both sides due to cratering on the front face of the panel, spalling of concrete on the back face of the panel, and/or perforation of the panel by the penetrator. All but one of the experiments had an impact velocity within 2.5 percent of the desired 1067 m/sec, and that one test (Test #12) was approximately 4.0 percent low at 1019 m/sec. Three of the tests (11, 27, and 43) had the residual screens tripped by material spalling off the backside of the panel and, therefore, did not record a residual FSP velocity.

The damage states, or responses, of the panels were consistent across the different fiber types. The FSP perforated through each of the panels that had thicknesses of 25 and 50 mm (1.0 and 2.0 in.). An impact crater and significant backside spall was created for each of the 63-mm. (2.5-in.) thick panels. For each of the 76-mm. (3.0-in) thick panels, a smaller impact side crater was generated, and minimal, if any, backside damage was visible.

Figure 13 contains the averaged residual velocities for the 25-mm (1.0- in.) thick panels with the different fiber types. While the differences were not large, the panels made with 6-mm fibers generally produced a lower residual velocity for both the 25-mm and 50-mm panel thicknesses. Since the FSP did not perforate through any of the 63- or 76-mm (2.5- or 3.0-in.)-thick panels, there were no residual velocities for those cases.

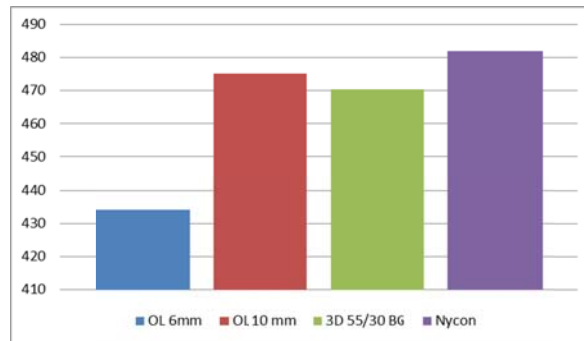


Figure 13. Average residual velocities (m/s) for 25-mm (1.0-in.) thick panels.

Loss of weight due to the damage ranged from 0.75 percent to 5.5 percent over the series of experiments, which is shown in Figure 15. Although the 25-mm (1.0-in.) panels were perforated, they had a smaller percentage of weight loss than the 50- or 63-mm- (2.0- or 2.5-in.) thick panels. The 76-mm (3.0-in.) panels exhibited the least loss of mass due to having only smaller impact side craters.

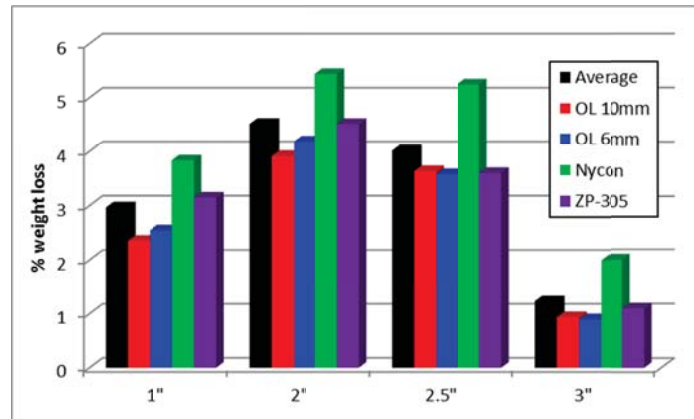


Figure 15. Percent weight loss for each fiber type and panel thickness.

## 5 Summary and Conclusions

The overall goal of this effort was to provide a better understanding of the effect of fiber size and shape on the response of UHPC at quasi-static and dynamic rates of loading. The testing utilized a laboratory standard UHPC known as Cor-Tuf Baseline (CT) that was produced using four fiber types: Bekaert 3D 55/30 BG (in the standard CT formulation), Nycon Type V, Bekaert OL 0.2/10 mm, and Bekaert OL 0.16/6 mm. Based on the results of the experimental investigation, the following conclusions were made:

Fiber size and shape have a negligible impact on compressive strength. This result was anticipated as compressive properties are more strongly correlated with the properties of the matrix than of the fiber reinforcement, which is provided to improve the tensile properties.

The results of flexural and direct tensile testing showed a strong impact of fiber dimensions and shape. Smaller fibers, such as the 6-mm OL fibers, provided a significant increase in tensile strength, stress vs. strain linearity, and toughness. As fiber sizes increased, tensile strengths generally decreased. Even with their reduced strength, specimens made with the larger 3D 55/30 BG and Nycon Type V fiber did exhibit some post-yield load carrying capacity. The results indicated that the smaller OL fibers significantly improved properties and limited damage and nonlinearity prior to reaching the ultimate strength. Once damage was initiated, the larger fibers were more effective at bridging larger cracks and redistributing stresses.

The dynamic response of specimens impacted with FSPs provided similar relationships between fiber size and response. The smaller OL fibers were more effective in reducing residual velocities of projectiles and minimizing mass loss due to cratering and/or spallation. Large fibers exhibited higher residual velocities and more extensive damage on the impact and exit faces of UHPC panels. Fiber size and shape did not have a significant impact on whether or not a panel was perforated during testing, as all UHPC-fiber combinations transitioned from a non-perforated to a perforated state at the 50- to 63-mm (2.0- to 2.5-in.) panel thickness transition.

The primary conclusion from this research was that fiber size and shape do have a significant impact on both quasi-static and dynamic properties of UHPCs. Given the fact that fiber dosage rates were made on a percentage basis, the number density of fibers also has a significant impact on correlations between fiber type and UHPC response. This is likely one of the primary reasons that smaller OL fibers performed significantly better in most tests than their larger counterparts. Another issue encountered was that larger fibers require larger test articles in order to uniformly distribute the fibers and minimize preferential fiber orientation. This was an issue in the direct tensile testing that required a specimen with limited cross-sectional area in the gage length.

## 6 References

1. ASTM International. 2010a. *Standard test method for compressive strength of concrete cylinders cast in place in cylindrical molds*. Designation: C872/873M. West Conshohocken, PA:ASTM International. doi: 10.1520/C0873\_C0873M-10A. [www.astm.org](http://www.astm.org).
2. \_\_\_\_\_. 2010b. *Standard test method for static modulus of elasticity and Poisson's ratio of concrete in compression*. Designation: C469/496M. West Conshohocken, PA:ASTM International. doi: 10.1520/C0469\_C0469M-10. [www.astm.org](http://www.astm.org).
3. \_\_\_\_\_. 2011. *Standard test method for splitting tensile strength of cylindrical concrete specimens*. Designation: C 496/496M. West Conshohocken, PA:ASTM International. doi: 10.1520/C0496\_C0496M-11. [www.astm.org](http://www.astm.org).
4. \_\_\_\_\_. 2012. *Standard test method for flexural performance of fiber-reinforced concrete (using beam with third-point loading)*. Designation: C1609/1609M. West Conshohocken, PA: ASTM International. doi: 10.1520/C1609\_C1609M-12. [www.astm.org](http://www.astm.org).
5. \_\_\_\_\_. 2013. *Standard practice for making and curing concrete test specimens in the laboratory*. Designation: C 192/192 M. West Conshohocken, PA: ASTM International. doi: 10.1520/C0873\_C0873M-10A. [www.astm.org](http://www.astm.org).
6. Burroughs, J.F.; Rushing, T.S.; Boone, N.; and Magee, R.E. Jr. 2013. Physical Property Influence on Ballistic Resistance of Ultra-High Performance Concrete Panels. Technical Report ERDC/GSL TR-13-4. Vicksburg, MS: U.S. Army Engineer Research and Development Center.
7. Green, B., R. Moser, D. Scott, and W. Long. 2014. Ultra-high performance concrete history and usage by the United States Army Engineer Research and Development Center. ASTM C09 Symposium on Ultra-High Performance Concrete; ASTM Special Technical Publication 1581, 2014. *ASTM Journal of Advances in Civil EngineeringMaterials*
8. Japanese Society of Civil Engineers (JSCE). 2008. *Recommendations for design and construction of high performance fiber reinforced cement composites with multiple fine cracks*. Tokyo: Japan Society of Civil Engineers.
9. O'Neil, E. F. 2008. *On engineering the microstructure of high-performance concretes to improve strength, rheology, toughness, and frangibility*. PhD diss., Northwestern University, Evanston, IL.
10. Reinhart, W. D., and T. F. Thornhill III. 2010. *Ballistic penetration test results for ductal and ultra-high performance concrete samples*. SAND2010-2222. Albuquerque, NM: Sandia National Laboratories.
11. Roth, Jason M., S. T. Rushing, G. O. Flores, D. Sham, and J. W. Stevens. 2010. *Laboratory investigation of the characterization of Cor-Tuf flexural and splitting tensile properties*. ERDC/GSL-TR-10-46. Vicksburg, MS: U.S. Army Engineer Research and Development Center.
12. Williams, E.M., S. S. Graham, P. A. Reed, and T. S. Rushing. 2009. *Laboratory Characterization of Cor-Tuf Concrete With and Without Steel Fibers*. Technical Report ERDC/GSL TR-09-22. Vicksburg, MS: U.S. Army Engineer Research and Development Center.
13. Williams, B. A. (2015). *Equipment and protocols for quasi-static and dynamic tests of High-Strength High-Ductility Concrete (HSHDC) and Very-High-Strength Concrete (VHSC)*. (Masters Thesis). Mississippi State University.

## 7 Acknowledgements

This study was conducted for the Technical Support Working Group (TSWG). The technical monitor was James L. O’Daniel.

The work was performed by the Concrete and Materials Branch (CMB) of the Engineering Systems and Materials Division (ESMD) and Structural Mechanics Branch (SMB) of Geosciences and Structures Division (GSD), U.S. Army Engineer Research and Development Center, Geotechnical and Structures Laboratory (ERDC-GSL). At the time of publication, Christopher M. Moore was Chief, CMB; Dr. William Gordon McMahon was Chief, ESMD; and Pamela Kinnebrew was the Technical Director for Military Engineering. The Deputy Director of ERDC-GSL was Dr. William P. Grogan, and the Director was Bartley P Durst.

Colonel Bryan Green was the Acting Commander of ERDC, and Dr. Jeffery P. Holland was the Director.